INTERNATIONAL JOURNAL OF ADAPTIVE CONTROL AND SIGNAL PROCESSING, VOL. 9, 301–324 (1995)

# GODARD BLIND EQUALIZER ERROR SURFACE CHARACTERISTICS: WHITE, ZERO-MEAN, BINARY SOURCE CASE

C. RICHARD JOHNSON JR.

*School of Electrical Engineering, Engineering and Theory Center, Cornell University, Ithaca, NY 14853, U.S.A.*

AND

BRIAN D. O. ANDERSON

*Department of Systems Engineering and the Cooperative Research Centre for Robust and Adaptive Systems, Australian National University, Canberra, A.C.T. 0200, Australia*

SUMMARY

We study the Godard/CMA error surface in adapting the impulse response coefficients of a finite-length, tapped-delay-line filter to equalize a white, zero-mean, binary ($\pm 1$) source that suffers ISI due to a linear channel. Our results arise primarily from examination of the expressions for the gradient and the Hessian in the baud-spaced equalizer parameter space of the cost-function in this particular setting. This paper presents results useful in topological assessment of procedures for initializing a gradient descent algorithm on this multimodal surface in the equalizer parameter space.

KEY WORDS: blind adaptive equalization; Godard algorithm; CMA algorithm; multimodal cost function stationary point analysis

## 1. INTRODUCTION

'You have the ability to adapt to diverse situations'.

Chinese Fortune Cookie

What is now referred to as the Godard (or constant modulus) algorithm for blind equalization was introduced in References 1 and 2. In Reference 1 the possibility of false minima is suggested. A false minimum is a local minimum of the Godard cost function in the equalizer parameter space that does not provide globally optimal performance. A large enough initialization of the reference (or centre) tap, with all others set to zero, is suggested in Reference 1 as a method of avoiding attraction to a false minimum by a doubly-infinite-length, tapped-delay-line equalizer.

In References 3 and 4 the convergence to globally optimal performance in the recovery of a white source by the Godard algorithm was proven from any initial parametrization of a doubly-infinite-length, baud-spaced, tapped-delay-line equalizer. The supporting analysis in References 3 and 4 can be viewed as an evaluation of the extremal properties of the performance function in the parameter space formed by the impulse response coefficients of the series combination of the channel and equalizer. When the equalizer itself is infinite-dimensional, so is the combined

CCC 0890–6327/95/040301–24

*Received 2 February 1994*
*Revised 25 November 1994*

channel–equalizer parameter space, and a linear (convolutional) similarity transformation exists that assures that the extremal properties in the combined equalizer–parameter space carry over to the equalizer-only parameter space. This invertible relationship is lost once the equalizer is finite in length. However, one might infer (and Reference 3 suggests that the inference is valid) that the Godard algorithm would retain this powerful global convergence property, i.e. asymptotic optimality from any equalizer initialization, if it were adjusting a finite-length, tapped-delay line that was long enough, possibly with the addition of some modest modification to the Godard algorithm. The modifications suggested in Reference 3 are intended to keep the centre of gravity of the equalizer weights near the centre of the equalizer tapped-delay line, as befits a truncated and delayed two-sided approximation to the inverse of the finite-impulse response of a linear channel with zeros inside and outside the unit circle.

*Unfortunately, global asymptotic optimality is not always a feature of the (unrefined) Godard algorithm when applied to a finite-length equalizer long enough to provide an accurate model of the channel inverse.* Consider an equalizer tapped-delay-line length long enough, if appropriately parametrized, to provide a perfect match to the FIR dynamics of the inverse of an AR channel. As shown in Reference 5, false minima can exist. Furthermore,[6] because these false minima can possess non-vanishing local curvature, no tapped-delay-line equalizer of finite length is long enough to guarantee convergence to optimal performance from all possible initializations of the (unrefined) Godard algorithm. A nullspace interpretation (which is a critical element of our analytical approach here) of such false minima of the Godard algorithm is provided in Reference 7. For a tutorial review of this admissibility question for finite-length blind equalizers of the memoryless error function class see Reference 8. A more recent survey exploring blind equalization research, including the admissibility issue, appears in Reference 9.

Proofs of admissibility of finite-length blind equalizers in current use under broad operating conditions remain sadly lacking. However, there is no lack of confidence that a pragmatic initialization will prove to result in global asymptotic optimality. For example, as stated in Reference 10 (p. 31): 'No doubt we can get into trouble with short equalizers, or initializing the equalizer with the central tap at one end while the channel is asking for taps beyond it to be equalized. Yet, since we know this fact, we should be able to avoid it'.

Previous research has only begun to consider under what sets of conditions (including channel and source restrictions, special initialization procedures and algorithm modifications) asymptotic global optimality is actually retained by finite-length Godard blind equalizers. In this paper we will enter this issue by restricting our interest to

(a) a linear, finite-impulse-response channel
(b) a white, zero-mean, binary ($\pm 1$) source
(c) a linear, baud-spaced, finite-impulse-response, tapped-delay-line equalizer
(d) an (unrefined) Godard algorithm (i.e. CMA(2, 2)).

Our objective in this paper is to add to a characterization of the associated Godard/CMA cost function surface in the finite-dimensional equalizer parameter space in a manner that assists the assessment of the utility of various equalizer parameter initialization procedures.

The next section describes the equalizer system of interest. Section 3 derives useful formulae for the gradient, Hessian and gradient descent dynamics of the Godard cost function in the equalizer parameter space. Averaging theory[11–13] establishes that with a suitably small step size and appropriate excitation, once the adaptive system parametrization from a stochastic gradient descent (as used in deriving CMA[2]) reaches the vicinity of a parametrization that zeros the gradient of the cost function and causes the associated Hessian to be positive definite, the adaptive system will hover about this local minimum of the cost function. Furthermore, the path

that the Godard algorithm takes from its initialization closely tracks the gradient descent path from that initialization on the associated error surface of the averaged system. The remainder of the body of the paper (i.e. Sections 4–6) is a collection of observations about the error surface of the Godard algorithm with a white, zero-mean, binary ($\pm 1$) source and a taped-delay-line channel model that arise from dissecting the formulae for the gradient, Hessian and average system gradient descent dynamics derived in Section 3. For example, we

(i) establish that motion along gradient descent paths sufficiently distant from the equalizer space origin moves closer to the origin
(ii) catalogue the various stationary points and establish for suitably long equalizers which subsets include all the maxima and all the false minima (if any exist)
(iii) establish the infinite extent of convex sets with a positive definite Hessian about any minimum, local or global.

A novelty here related to similar previous work, e.g. Reference 14, is our focus on properties of the gradient and Hessian of the Godard cost function.

## 2. PROBLEM SPECIFICATION AND APPROACH OVERVIEW

A linear equalizer plus non-linear memoryless decision device is illustrated in Figure 1. For a source sequence $s(k)$ composed of plus and minus ones, as is assumed here, the nearest element decision device is a sign operator. The linear equalizer is intended to cancel the dynamics of the linear channel by forming a delayed approximation of the two-sided inverse of the channel. As long as this delay is acceptable and the sign of the equalizer output sequence exactly matches the delayed binary source sequence value of $+1$ or $-1$, the communications system performance objective of an open-eye channel–equalizer combination is met. In fact, for typical differentially encoded sources, always matching the opposite of the sign of the source sequence is as satisfactory as always matching the sign of it. Thus the equalizer would be satisfactory in our case as long as it adequately approximated either the delayed two-sided inverse of the channel or the negative of the delayed two-sided inverse of the channel. In practice, improving the accuracy of this approximation will increase the degree of eye-opening, i.e. the tightness of the clustering of the equalizer output values about the locations of source alphabet members. Such a margin is important as a buffer against e.g. channel noise.

The closer any of the channel zeros are to the unit circle, the more terms are needed in a linear, tapped-delay-line equalizer to obtain a certain accuracy fit to the delayed two-sided inverse. Practically speaking, a linear, series-cancellation equalizer is inappropriate for a channel with deep nulls in its frequency response. Linear equalizers may also prove inadequate for channels with significant non-linearities. We assume that we are posing the problem implicit in Figure 1 only when it offers adequate performance for the length of equalizer selected and with the equalizer optimally tuned (with optimality based on globally minimizing the Godard cost function). A remaining significant practical issue with such a problem statement is the determination of an adaptive equalizer parameter initialization strategy.

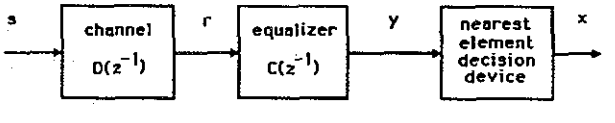


Figure 1. Linear dynamics equalization

In our abstraction of this problem the equalizer output $y$ is related to the source sequence $s$ via the impulse response coefficients $h_i$ of the linear, FIR channel–equalizer combination:

$$y(k) = \sum_{i=0}^{P} h_i s(k-i) \tag{1}$$

The received signal (or channel output) $r$ is related to the source sequence $s$ via the impulse response coefficients $d_i$ of the channel:

$$r(k) = \sum_{i=0}^{M} d_i s(k-i) \tag{2}$$

The equalizer output $y$ is related to the received signal $r$ via the impulse response coefficients $c_i$ of the equalizer:

$$y(k) = \sum_{i=0}^{N} c_i r(k-i) \tag{3}$$

The sample period in (1)–(3) matches the period between successive source bauds, e.g. $s(k)$ and $s(k-1)$. Thus (3) is termed a baud-spaced equalizer. The series connection of (2) and (3) illustrated in Figure 1 is equivalent to (1) with $P = M + N$. When we are considering the dynamic behaviour of the adaptive algorithm, the $c_i$ (and $h_i$, but not $d_i$) will receive a time index as well, e.g. $c_i(k)$.

The minimal acceptable performance objective is to open asymptotically to a suitable degree the eye of the closed-eye channel with the addition of the equalizer, thereby providing perfect, though delayed, source recovery with the output of the decision device. In some circumstances,[5] some local minima of the Godard cost function do not open the eye of the channel–equalizer combination. A more ambitious performance objective is to form a good approximation of a delayed version of the inverse of the channel $D^{-1}(z^{-1})$ (or $-D^{-1}(z^{-1})$) so that $y$ closely approximates a delayed version of $s$ (or the sequence $-s$) e.g. with a bit error rate within a particular tolerance. Such a good fit is equalizer-length-dependent.

Another description of desired performance is proposed in References 1 and 2: minimization of the Godard (or constant modulus) cost function

$$J = \mathrm{E}[(1 - y^2(k))^2] \tag{4}$$

by choice of the equalizer parameters $c_i$. The small-step-size, stochastic gradient descent scheme for reaching (the neighbourhood of) a local minimum of this cost function is the Godard (or constant modulus) algorithm

$$c_i(k+1) = c_i(k) - \frac{\mu}{4} \frac{\partial(1 - y^2(k))^2}{\partial c_i(k)} = c_i(k) + \mu r(k-i) y(k)(1 - y^2(k)) \tag{5}$$

where $\mu$ is a small positive step size.

In keeping with the stochastic gradient descent strategy, in (5) we take the gradient of the instantaneous performance function rather than of the expectation of this function, which is the 'true' cost function from (4) that we wish to minimize. This 'stochastic' approximation to the dynamics of the smooth gradient descent of (4) is a close fit when the step size is suitably small. Indeed, averaging theory[12,13] indicates that the locations where (5) hovers asymptotically, and the trajectories it takes to get there, can be closely approximated by the behaviour of the system

$$\gamma(k+1) = \gamma(k) + \mu R(\gamma(k)) \tag{6}$$

where the $\gamma_i(k)$ in $\gamma = [\gamma_0(k)\ \gamma_1(k)\ \ldots\ \gamma_N(k)]^T$ correspond to the 'average' $c_i$ and $R$ is the average of the update term of the vector version of (5),

$$R(\gamma(k)) = \mathrm{E}\{[r(k)\ r(k-1)\ \ldots\ r(k-N)]^T y(k)(1-y^2(k))\} \tag{7}$$

with $y$ obtained by freezing the $c_i$ in (3) at the values $\gamma_i(k)$. $R$ is the negative of the partial derivative vector (or gradient) of the actual cost function (4) in the equalizer parameter space rather than the instantaneous approximation used in (5). Thus, when this $R$ is zero, (6) ceases updating and we have reached a stationary point for the cost function of (4). (Only on average would (5) cease to update. In general, it will continue to rattle.) Because (6) constructs a steepest descent path on the cost function of (4), we can expect the real algorithm with satisfactorily small (but non-vanishing) step size $\mu$ to approximately track such a steepest descent path and to be captured in the vicinity of a stationary point of (4) (where the gradient, i.e. $-R$, is zero) if its local Hessian $(-\partial R/\partial\gamma)$ is positive definite. Averaging theory[12,13] confirms these expectations.

Thus our approach in this paper is based on examining (6) with $R$ computed as in (7) as the negative of the gradient of (4) in the equalizer parameter space. We shall dissect the structure of $-R$ (and its partial derivative with respect to the equalizer parameters, which is the Hessian of the cost function) for clues to generic features of the behaviour of (6). The next section details the gradient and the Hessian in the equalizer parameter space of the cost function of (4).

*Illustrative example*

Though we will focus primarily on results applicable to a tapped-delay-line equalizer of any finite length, we will use a two-parameter equalizer, i.e. $N = 1$ in (3), to illustrate some of our results. The test channel has impulse response coefficients in (2) of

$$d_0 = 0{\cdot}5, \qquad d_1 = -0{\cdot}3, \qquad d_2 = 0{\cdot}25 \tag{8}$$

The definition of the closed-eye measure of the channel in (1) for our binary source is $(\sum_i |h_i| - \max_i |h_i|)/(\max_i |h_i|)$. This measure should be less than one for a sign operator decision device to recover perfectly all source signals with a delay equal to that associated with the maximum magnitude element of the channel–equalizer impulse response sequence. Thus, because $|d_1| + |d_2| > |d_0|$ (where $\arg(\max|d_i|) = 0$), the channel in (8) alone is closed-eye. For each of the equalizer tap weights varying incrementally from $-2$ to $+2$, those settings resulting in an open-eye combination in (1) are indicated with pluses in Figure 2. Because the channel is closed-eye, neither axis in Figure 2 is in the eye-opening region marked with pluses, though the $c_0$-axis comes close.

The channel of (8) has the frequency response of Figure 3. With the equalizer constrained to two parameters it can locate one zero on the real axis in an attempt to convert the sum of the log-magnitude and phase curves of the frequency responses of the single zero and Figure 3 into an allpass. Thus we should expect an eye-opening equalizer to be a lowpass filter with the equalizer zero $-c_1/c_0$ on the negative portion of the real axis inside the unit circle or

$$1 > c_1/c_0 > 0 \tag{9}$$

which corresponds to the open-eye region of Figure 2. Both the Godard cost function and the open-eye measure are symmetrical about the origin of the equalizer parameter space.

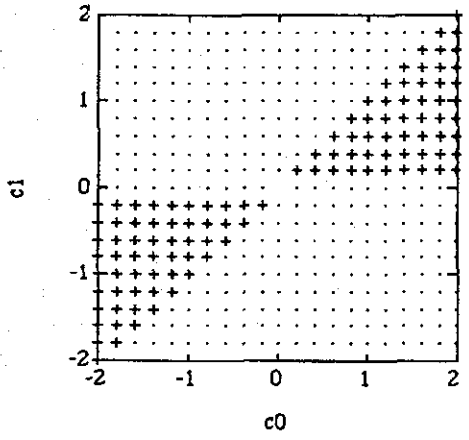


Figure 2. Open/closed-eye territory of illustrative example (+, open, ·, closed)

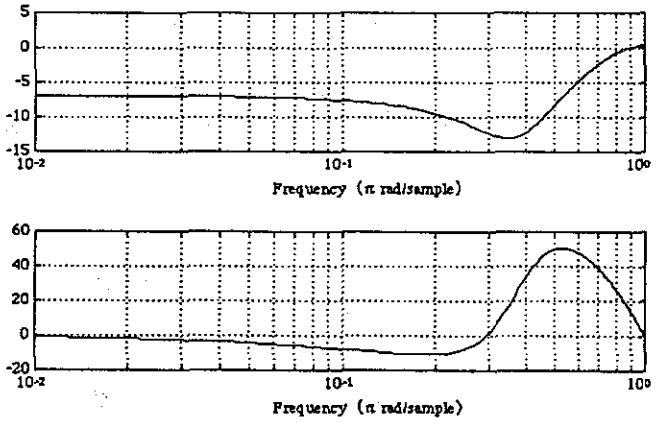


Figure 3. Example channel frequency response

## 3. THE KEY EQUATIONS: COST, GRADIENT AND HESSIAN

One property of a stochastic gradient descent algorithm as in (5) is that, for suitably small step size $\mu$, attractive points about which the algorithm hovers asymptotically are given by equalizer parametrizations that zero the gradient of the cost function in the equalizer parameter space and have a positive definite Hessian there.[12,13] Therefore in this section we are primarily interested in deriving the gradient $\partial J/\partial c_i$ and the Hessian $\partial^2 J/\partial c_l \partial c_m$ of the cost function in (4) given the relationship between $y$ and $s$ in (1)–(3).

We apologize in advance for sometimes speaking of average system behaviour but labelling it as adaptive system behaviour. As noted previously, this is only acceptable for some suitably small (but non-vanishing) step size in some average sense, which we will not further formalize in this paper. Instead, the interested reader is referred to Reference 12 or 13.

*Cost function*

Expanding (4) as

$$J = \mathrm{E}[(1 - y^2(k))^2] = 1 - 2\mathrm{E}[y^2(k)] + \mathrm{E}[y^4(k)] \tag{10}$$

we see that we need to assess $E[y^2(k)]$ and $E[y^4(k)]$. If, as in our case, $y$ is the output due to a white, zero-mean input of a system with impulse response coefficients $h_i$, then $E[y^2] = \sum_i h_i^2$. The evaluation of $E[y^4(k)]$ is a bit more involved.

We defined the source $s$ as a real sequence which is white and takes on the value $+1$ with probability 0·5 or the value $-1$ with the same probability. Thus for fixed $h_i$ form

$$E[y^4(k)] = \sum_{i=0}^{P}\sum_{j=0}^{P}\sum_{l=0}^{P}\sum_{m=0}^{P} h_i h_j h_l h_m \, E[s(k-i)s(k-j)s(k-l)s(k-m)] \tag{11}$$

Because $E[s(i)] = 0 \ \forall i$ and $E[s(i)s(j)] = 0$ for $i \neq j$, the only non-zero terms in the sum arise when the product of four values of $s$ at various times can be grouped into two pairs, i.e. $s(k-i)s(k-j)s(k-l)s(k-m) = s_1^2 s_2^2$ with $s_1 \neq s_2$ permitted. Exactly three groupings are possible from a set of four that gives a particular two pairs with different time arguments for the two pairs. For example, for the 4-tuple $(a, b, c, d)$ to have two different pairs, either $a = b$ (and $a \neq c = d$) or $a = c$ (and $a \neq b = d$) or $a = d$ (and $a \neq b = c$). However, only one possibility (i.e. $a = b = c = d$) has them all the same. Thus

$$E[y^4(k)] = 3\sum_{i=0}^{P}\sum_{j=0,\, j\neq i}^{P} h_i^2 h_j^2 \, E[s^2(k-i)s^2(k-j)] + \sum_{i=0}^{P} h_i^4 \, E[s^4(k-i)] \tag{12}$$

With $s(\cdot) = +1$ with probability 0·5 or $-1$ with probability 0·5, $E[s(\cdot)^2] = E[s(\cdot)^4] = 1$. Furthermore, because the $s(\cdot)$ are sequentially uncorrelated, $E[s^2(i)s^2(j)] = 1$ for $i \neq j$.

We use these observations to convert (10) to

$$J = 1 - 2\sum_{i=0}^{P} h_i^2 + 3\left[\sum_{i=0}^{P}\sum_{j=0,\, j\neq i}^{P} h_i^2 h_j^2\right] + \sum_{i=0}^{P} h_i^4 \tag{13}$$

The impulse response coefficients $h_i$ of the channel–equalizer series combination from (1)–(3) are the convolution of the channel $(d_i)$ and equalizer $(c_i)$ impulse response coefficients. Thus

$$h_j = \sum_{i=0}^{j} d_{j-i} c_i \tag{14}$$

for $j = 0, 1, 2, \ldots, P$. Recall that $d$ and $c$ take on non-zero values only for indices between 0 and $M$ and $N$ respectively, with $P = M + N$.

While (13) expresses $J$ as a function of the $h_i$, through (14) we can express it as a function of the $c_i$. We will discover that expressing $J$ (and subsequently its gradient and Hessian in the equalizer parameter space of the $c_i$) will be more convenient in terms of the $h_i$ rather than the $c_i$. However, we must not lose sight of the fact that, in formulating a gradient algorithm in the equalizer parameter space of the $c_i$, $J$ must be regarded as a function of the $c_i$.

For the illustrative example channel of (8) a contour plot of the resulting cost function is shown in Figure 4. Note the two false minima in the vicinity of $(c_0, c_1) = (0, \pm 1{\cdot}1)$. In this example the false minima are local minima that not only have suboptimal performance but also leave the eye of the channel–equalizer combination closed. These false minima have substantial regions of attraction in the equalizer parameter space. The origin is a local maximum. The global minima in the vicinity of $\pm(1{\cdot}6, 0{\cdot}9)$ are within the eye-opening region shown in Figure 2.

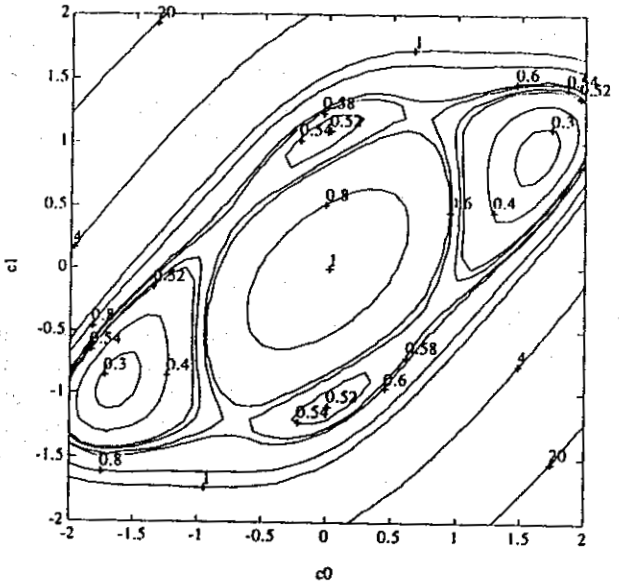


Figure 4. Contours of example cost function

*Gradient*

Given (13), to examine $\partial J/\partial c_i$, we need to evaluate

$$\frac{\partial(\sum_{j=0}^{P} h_j^4)}{\partial c_i} = 4\sum_{j=0}^{P} h_j^3 \frac{\partial h_j}{\partial c_i} = 4\sum_{j=0}^{P} h_j^3 d_{j-i} \tag{15}$$

The last step uses the fact arising from (14) that $\partial h_j/\partial c_i$ is simply $d_{j-i}$. However, $d_{j-i}$ is non-zero only if $j-i \geq 0$ ($\Rightarrow j \geq i$) and $j-i \leq M$ ($\Rightarrow j \leq M+i$). Thus (15) can be written as

$$\frac{\partial(\sum_{j=0}^{P} h_j^4)}{\partial c_i} = 4\sum_{j=0}^{M+i} h_j^3 d_{j-i} \quad \text{for } i = 0, 1, 2, \ldots, N \tag{16}$$

We also need to evaluate

$$\frac{\partial(\sum_{j=0}^{P} h_j^2)}{\partial c_i} = 2\sum_{j=0}^{P} h_j \frac{\partial h_j}{\partial c_i} = 2\sum_{j=i}^{M+i} h_j d_{j-i} \tag{17}$$

and, when $j \neq l$ so $h_j h_l \neq h_j^2$,

$$\begin{aligned}\frac{\partial(\sum_{j=0}^{P}\sum_{l=0,l\neq j}^{P} h_j^2 h_l^2)}{\partial c_i} &= \sum_{j=0}^{P} h_j^2 \frac{\partial(\sum_{l=0,l\neq j}^{P} h_l^2)}{\partial c_i} + \sum_{l=0}^{P} h_l^2 \frac{\partial(\sum_{j=0,j\neq l}^{P} h_j^2)}{\partial c_i} \\ &= 2\sum_{j=0}^{P} h_j^2 \sum_{l=i,l\neq j}^{M+i} h_l d_{l-i} + 2\sum_{l=0}^{P} h_l^2 \sum_{j=i,j\neq l}^{M+i} h_j d_{j-i} \\ &= 4\sum_{l=0}^{P} h_l^2 \sum_{j=i,j\neq l}^{M+i} h_j d_{j-i}\end{aligned} \tag{18}$$

Using (16)–(18) in $J$ from (13) yields

$$\frac{\partial J}{\partial c_i} = -2\left(2\sum_{j=i}^{M+i} h_j d_{j-i}\right) + 3\left(4\sum_{l=0}^{P} h_l^2 \sum_{j=i,\, j\neq l}^{M+i} h_j d_{j-i}\right) + \left(4\sum_{j=i}^{M+i} h_j^3 d_{j-i}\right)$$

$$= \sum_{j=i}^{M+i}\left(12\sum_{l=0}^{P} h_l^2 - 4 - 8h_j^2\right) h_j d_{j-i} \tag{19}$$

With the definition

$$\Lambda_j = 4\left(3\sum_{l=0}^{P} h_l^2 - 1 - 2h_j^2\right) \tag{20}$$

we can write

$$\frac{\partial J}{\partial c_i} = \sum_{j=i}^{M+i} \Lambda_j h_j d_{j-i} \tag{21}$$

Direct calculation from (13) or interpretation of (21) via $\partial J/\partial c = (\partial J/\partial h)(\partial h/\partial c)$ reveals $\Lambda_j h_j$ as $\partial J/\partial h_j$.

Concatenate (21) for each $i = 0, 1, \ldots, N$ to describe the requirement for a stationary point as

$$\begin{bmatrix} \left(\frac{\partial J}{\partial c_0}\right) \\ \left(\frac{\partial J}{\partial c_1}\right) \\ \vdots \\ \left(\frac{\partial J}{\partial c_N}\right) \end{bmatrix} = \begin{bmatrix} d_0 & d_1 & \cdots & d_M & 0 & 0 & \cdots & 0 \\ 0 & d_0 & \cdots & d_{M-1} & d_M & 0 & \cdots & 0 \\ \vdots & \ddots & \ddots & & \ddots & \ddots & \ddots & \vdots \\ 0 & \cdots & 0 & d_0 & \cdots & d_{M-1} & d_M & 0 \\ 0 & \cdots & \cdots & 0 & d_0 & \cdots & d_{M-1} & d_M \end{bmatrix} \begin{bmatrix} \Lambda_0 h_0 \\ \Lambda_1 h_1 \\ \vdots \\ \Lambda_{M+N-1} h_{M+N-1} \\ \Lambda_{M+N} h_{M+N} \end{bmatrix}$$

$$= 0 \tag{22}$$

With the definition of the $(M+N+1) \times (N+1)$ matrix

$$\Delta = \begin{bmatrix} d_0 & d_1 & \cdots & d_M & 0 & 0 & \cdots & 0 \\ 0 & d_0 & \cdots & d_{M-1} & d_M & 0 & \cdots & 0 \\ \vdots & \ddots & \ddots & & \ddots & \ddots & \ddots & \vdots \\ 0 & \cdots & 0 & d_0 & \cdots & d_{M-1} & d_M & 0 \\ 0 & \cdots & \cdots & 0 & d_0 & \cdots & d_{M-1} & d_M \end{bmatrix}^{\mathrm{T}} \tag{23}$$

the $(P+1) \times (P+1)$ diagonal matrix

$$\Lambda = \mathrm{diag}[\Lambda_0 \ \Lambda_1 \ \cdots \ \Lambda_P] \tag{24}$$

where $P = M + N$ and $\Lambda_j$ is defined by (20), the $(P+1) \times 1$ vector

$$h = [h_0 \ h_1 \ \cdots \ h_P]^{\mathrm{T}} \tag{25}$$

and the $(N+1) \times 1$ vector

$$c = [c_0 \ c_1 \ \cdots \ c_N]^{\mathrm{T}} \tag{26}$$

the gradient of (22) can be rewritten in matrix form as

$$\frac{\partial J}{\partial c} = \Delta^T \Lambda h \tag{27}$$

and the combined channel–equalizer impulse response coefficients of (14) as

$$h = \Delta c \tag{28}$$

Recall $-R$ in (6) and (7). The stationary points of the Godard cost function $J$ are defined by zeroing the gradient

$$\Delta^T \Lambda h = \Delta^T \Lambda \Delta c = 0 \tag{29}$$

To help characterize the update trajectory from our form of the gradient in (27), for the illustrative example channel parametrized in (8), we decompose the algorithm motion (in the negative of the gradient direction) into a radial component and an angular component in Figures 5 and 6. A plus in Figure 5 indicates radial motion away from the origin. A dot

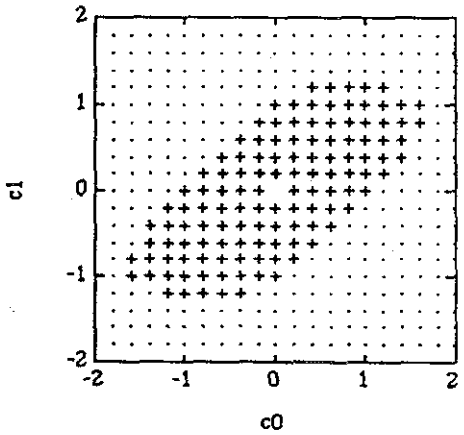


Figure 5. Radial motion component (+, outwards; ·, inwards)

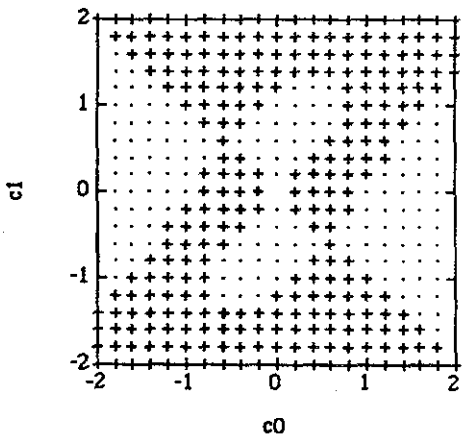


Figure 6. Angular motion component (+, clockwise; ·, counterclockwise)

indicates radial motion towards the origin. In Figure 6 a plus (dot) indicates clockwise (counterclockwise) rotation by subsequent gradient descent. (The upward gradient, being the negative of the motion, would use the reversed definitions of pluses and dots.) The minima and saddle points in Figure 4 correspondingly exist where the boundary between clockwise and counterclockwise motion intersects the boundary between radial inward and outward motion. These pictures will prove helpful later in confirming our subsequent analytical results.

*Hessian*

For a candidate stationary point of the average system, for which $\partial J/\partial c_i = 0$ for all $i = 0, 1, \ldots, N$, to be stable, the Hessian (the $ij$th element of which is $\partial^2 J/\partial c_i \partial c_j$) must be positive definite. We shall now obtain a useful expression for the Hessian.

Using (17) and (19),

$$\begin{aligned}\frac{\partial^2 J}{\partial c_i^2} &= \sum_{j=i}^{M+i} \frac{\partial}{\partial c_i}\left(-4h_j + 12h_j \sum_{l=0}^{P} h_l^2 - 8h_j^3\right) d_{j-i} \\ &= \sum_{j=i}^{M+i}\left(-4d_{j-i} + 12\frac{\partial h_j}{\partial c_i}\sum_{l=0}^{P} h_l^2 + 12h_j \sum_{l=0}^{P}\frac{\partial}{\partial c_i} h_l^2 - 24h_j^2 d_{j-i}\right) d_{j-i} \\ &= \sum_{j=i}^{M+i}\left(-4d_{j-i}^2 + 12d_{j-i}^2 \sum_{l=0}^{P} h_l^2 + 24h_j d_{j-i} \sum_{l=i}^{M+i} h_l d_{l-i} - 24h_j^2 d_{j-i}^2\right) \end{aligned} \tag{30}$$

and similarly for $i \neq m$

$$\frac{\partial^2 J}{\partial c_i \partial c_m} = \sum_{j=i}^{M+i}\left(-4d_{j-i}d_{j-m} + 12d_{j-i}d_{j-m}\sum_{l=0}^{P} h_l^2 + 24h_j d_{j-i}\sum_{l=i}^{M+i} h_l d_{l-m} - 24h_j^2 d_{j-i}d_{j-m}\right) \tag{31}$$

Given the definitions (20), (23) and (24), we collect (30) and (31) into a matrix expression

$$\begin{bmatrix} \frac{\partial^2 J}{\partial c_0 \partial c_0} & \frac{\partial^2 J}{\partial c_0 \partial c_1} & \cdots & \frac{\partial^2 J}{\partial c_0 \partial c_N} \\ \frac{\partial^2 J}{\partial c_1 \partial c_0} & \frac{\partial^2 J}{\partial c_1 \partial c_1} & \cdots & \frac{\partial^2 J}{\partial c_1 \partial c_N} \\ \vdots & \vdots & \ddots & \vdots \\ \frac{\partial^2 J}{\partial c_N \partial c_0} & \frac{\partial^2 J}{\partial c_N \partial c_1} & \cdots & \frac{\partial^2 J}{\partial c_N \partial c_N} \end{bmatrix} = \Delta^{\mathrm{T}} \Psi \Delta \tag{32}$$

where

$$\Psi = \left(12\sum_{l=0}^{P} h_l^2 - 4\right) I_{M+N+1} + 24\begin{bmatrix} h_0 \\ h_1 \\ \vdots \\ h_{M+N} \end{bmatrix} [h_0 \;\; h_1 \;\ldots\; h_{M+N}] - 24\,\mathrm{diag}([h_0^2 \;\; h_1^2 \;\ldots\; h_{M+N}^2]) \tag{33}$$

where $I_{M+N+1}$ is an $(M+N+1) \times (M+N+1)$ identity matrix. An alternative derivation of (32)–(33) can be achieved via partial derivation of the gradient vector in (27)–(28) and

$\partial(\Delta^T \Lambda h)/\partial c = \Delta^T(\partial(\Lambda h)/\partial h)(\partial h/\partial c)$, with $\Psi$ in (33) revealed as $\partial(\Lambda h)/\partial h$. Recall (20) and (24), which indicate that $\Lambda$ is a function of $h$, so $\partial(\Lambda h)/\partial h = \Psi \neq \Lambda$.

The signs of the eigenvalues of the Hessian for the illustrative example of (8) are indicated in Figure 7. A plus indicates a positive definite Hessian, which is needed for a local minimum. Note how the global and local minima in Figure 2 fall in such regions. A Hessian with one positive and one negative eigenvalue is indicated by a dot. An indefinite Hessian at a stationary point indicates that it is a saddle point. No marking indicates a negative definite Hessian required for a local maximum. The negative definite region surrounds the origin of the equalizer parameter space in Figure 7, as expected given the local maximum at the origin.

*Recap*

The key equations from this section are the compact descriptions of the gradient vector (from (27))

$$\boxed{\frac{\partial J}{\partial c_i} = \Delta^T \Lambda h} \tag{G}$$

the Hessian matrix (from 32))

$$\boxed{\frac{\partial^2 J}{\partial c_i \partial c_j} = \Delta^T \Psi \Delta} \tag{H}$$

and the 'average' system (from substitution of (G) given (28) for $-R$ in (7))

$$\boxed{\gamma(k+1) = [I - \mu \Delta^T \Lambda(k) \Delta]\gamma(k)} \tag{AS}$$

The $\gamma_i$ in (AS) approximate the average behaviour of the $c_i$. Thus, to connect (G) and (H) to (AS), use $h(k) = \Delta\gamma(k)$. This definition of $h$ should also be used in defining $\Lambda$ and $\Psi$ in (24) (using (20)) and (33) respectively. The banded matrix $\Delta$ defined in (23) is composed from the channel impulse response coefficients $d_i$.

In the remainder of this paper we shall establish a number of properties of (AS).

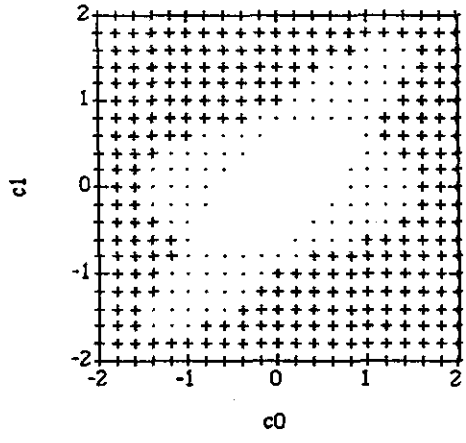


Figure 7. Hessian: two positive eigenvalues (+); one positive (·)

## 4. CONTRACTION AND EXPANSION

*For parametrizations sufficiently distant from the origin of tapped-delay-line equalizers of finite length, the Godard cost function is shaped so that motion along any gradient descent path decreases the distance to the origin. Conversely, for all equalizer parametrizations sufficiently near the origin, motion along gradient descent paths increases the distance from the origin.*

In this section we will establish the preceding observation by examining $\gamma^T(k+1)\gamma(k+1) - \gamma^T(k)\gamma(k)$ from (AS). When $\Lambda$ is positive definite, because $\Lambda$ is diagonal, the quadratic form of $\Delta^T\Lambda\Delta$ will be positive definite. Thus, if $\mu$ is chosen small enough, the eigenvalues of $I - \mu\Delta^T\Lambda(k)\Delta$ in (AS) will all be less than unity in magnitude and $\gamma^T(k+1)\gamma(k+1)$ will be smaller than $\gamma^T(k)\gamma(k)$. If $\mu$ is less than two divided by the largest eigenvalue of $\Delta^T\Lambda(k)\Delta$, (AS) is a contraction.

Contraction of (AS) continues until one or more entries in the diagonal $\Lambda(k)$ reach (or goes below) zero. From (20), with $h = \Delta\gamma$ we see that the smallest diagonal entry in $\Lambda$ occurs with the largest $|h_i|$. With the largest $|h_i|$ occurring for $i = I$, the contraction continues just as long as

$$3\sum_{l=0}^{P} h_l^2(k) - 1 - 2h_I^2(k) > 0 \tag{34}$$

or

$$h_I^2(k) + 3\sum_{l=0,\, l\neq I}^{P} h_l^2(k) > 1 \tag{35}$$

Because (35) must be dissatisfied at all stationary points, (35) establishes an upper bound on the asymptotic $\|h\|$ and thus on the asymptotic $\|\gamma\|$ (or average $\|c\|$). For example,

$$\sum_{l=0}^{P} h_l^2(k) > 1 \tag{36}$$

results in satisfaction of (35). Using $h = \Delta\gamma$, (36) becomes

$$\gamma^T\Delta^T\Delta\gamma > 1 \tag{37}$$

Because $\Delta^T\Delta$ is a positive definite matrix, $\lambda_{\min}(\Delta^T\Delta) > 0$ and for all $\gamma$ sufficiently far from the origin such that

$$\gamma^T\gamma > [\lambda_{\min}(\Delta^T\Delta)]^{-1} \tag{38}$$

$\Lambda$ will be positive definite.

Using similar arguments to those preceding (34), as long as $h \neq 0$ and

$$3\sum_{l=0}^{P} h_l^2(k) - 1 - 2h_i^2(k) < 0 \quad \forall i \tag{39}$$

$\|\gamma\|$ expands. This inequality is satisfied if

$$\sum_{l=0}^{P} h_l^2(k) < \tfrac{1}{3} \quad \forall i \tag{40}$$

Thus, with the set about the origin in the equalizer parameter space that results in satisfaction of (40), (AS) results in $\gamma^T(k+1)\gamma(k+1) > \gamma^T(k)\gamma(k)$ as long as $\gamma(k) \neq 0$. Similarly to (36) and (37), inequality (40) implies that

$$\gamma^T \Delta^T \Delta \gamma < \tfrac{1}{3} \tag{41}$$

which is implied by

$$\gamma^T \gamma < \tfrac{1}{3}[\lambda_{max}(\Delta^T \Delta)]^{-1} \tag{42}$$

For a white source, satisfaction of the condition in (36) indicates that contraction continues as long as the variance of the equalizer output is greater than the desired modulus or that no stationary points can have the variance of the equalizer output greater than the desired modulus. This is consistent with the properties noted in Sect. II-D of Reference 5 and Sect. 3.3 of Reference 14, which indicate that no local minima are possible that satisfy (36). Combining this observation with (38), (40) and (42) and relating $\gamma$ to the average $c$, we can state that local minima are possible in the equalizer parameter space only in the region described by

$$[\lambda_{min}(\Delta^T \Delta)]^{-1} > c^T c > \tfrac{1}{3}[\lambda_{max}(\Delta^T \Delta)]^{-1} \tag{43}$$

For our white, binary, zero-mean, $\pm 1$ source, $\Delta^T \Delta$ is the autocorrelation matrix of the received signal $r$.[15] As noted in Reference 16, with an increasing number of data points, i.e. increasing filter length, the extreme eigenvalues of such an autocorrelation matrix approach the extreme values of the signal spectrum. Thus (43) indicates that the upper and lower bounds of the received signal spectrum can be used to upper and lower bound all locally optimal equalizer settings.

In Figure 8 the contraction test of (35) for the illustrative example of (8) is satisfied at locations marked by pulses. The expansion test of (39) is satisfied at locations marked by dots. As expected, the sharp boundary in Figure 5 falls within the wider one in Figure 8. Comparison with the cost function contours in Figure 4 indicates that for a sufficiently large equalizer parametrization the equalizer parameter vector norm contracts until reaching the vicinity of the last contour line that encloses all four minima.

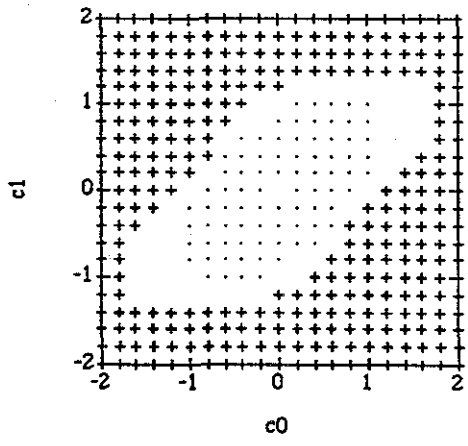


Figure 8. Contraction test satisfied (+); expansion test satisfied (·)

## 5. CATALOGUING STATIONARY POINTS

*For sufficiently long equalizers, stationary points can be divided into three broad classes. One is the solitary local maximum. Another includes only global minima and saddle points. The third includes all the false minima.*

We will define three classes of stationary points based on three possible ways in which the gradient formula of (G) is zeroed:

(i) $h = 0$
(ii) $\Lambda h = 0$ (with $h \neq 0$)
(iii) $\Lambda h$ exists in the nullspace of $\Delta$ (with $\Lambda h \neq 0$).

We will name these classes the *maxima class*, the *Mazo class* and the *Ding class* respectively in the light of earlier work. In this section we isolate characteristics of each of these classes.

We add, for just this section, to the assumptions (a)–(d) in Section 1 a further assumption:

(e) the channel transfer function has no zeros on the unit circle and the equalizer length is significantly larger than that required of an equalizer which approximates closely a (delayed) inverse of the channel.

The exclusion of channel zeros on the unit circle is a standard assumption of linear equalization to avert attempting to effectively place an equalizer 'pole' on the unit circle, which would require infinitely many taps in an FIR tapped-delay-line equalizer and would unacceptably amplify channel noise at that frequency. We implicitly included this requirement with our statement in Section 2 that we would be considering only those circumstances for which a finite-length equalizer could provide adequate performance.

To help understand the significance of the assumption of 'excessive' equalizer length, which is related to how close channel zeros can be to the unit circle, recall (2), which indicates that the channel transfer function is $D(z^{-1}) = d_0 + d_1 z^{-1} + \ldots + d_M z^{-M}$. Owing to the assumption that $D(z^{-1})$ has no roots on the unit circle, we can write

$$(d_0 + d_1 z^{-1} + \cdots + d_M z^{-M})^{-1} = \sum_{\alpha=-\infty}^{\infty} x_\alpha z^{-\alpha} \tag{44}$$

with $|x_\alpha| \to 0$ as $|\alpha| \to \infty$. This decay in $|x_\alpha|$ indicates that

$$(d_0 + d_1 z^{-1} + \cdots + d_M z^{-M})^{-1} \approx \sum_{\alpha=-Q}^{Q} x_\alpha z^{-\alpha} \tag{45}$$

for some $Q$ and all $z = \exp(j\omega)$, $0 \leq \omega \leq \pi$. Assumption (e) means that the equalizer length is several times the finite $2Q + 1$.

A consequence of assumption (e) is that there exist equalizer settings which can achieve a great variety of specified combined responses $h$. For example, suppose $\chi$ denotes the impulse response of an equalizer serving as an approximate delayed inverse of the channel with impulse response $d$. Then the equalizer $\chi * h$ (where '$*$' indicates convolution) will approximately produce a combined response with the channel $d$ that is a delayed version of $h$ with the same delay as that associated with the approximate inverse. The support of $h$ must be such that $\chi * h$ can be encompassed by the equalizer length, which by assumption (e) will be well in excess of that required just to implement the approximate delayed inverse of $d$, i.e. $\chi$. This support range constraint on $h$ connects to our sufficient equalizer length requirement in terms of the accuracy of invertibility needed to effect a particular $h$. The implicit approximations that result in e.g. stationary point locations are readily absorbed in a robust average system setting.[12,13] Thus our

presumption of the results being descriptive of finite-length adaptive filter behaviour can be maintained.

*Maxima class*

*The equalizer space origin is the only local maximum of the Godard cost function.*

A zero equalizer setting sets $h$ to zero. When $h$ is zeroed, $\Psi$ in (33) reduces to $-4I$. Therefore the Hessian in (H) is negative definite. Thus the origin of the equalizer space (or $h=0$) corresponds to a local maximum.

However, is the origin of the equalizer parameter space the only local maximum? If it were not, another stationary point with a non-zero $h$ (under the assumption of a non-zero $\Delta$) would exist for which $\Psi$ in (33) would be negative definite. This cannot happen.

For $\Psi$ to be negative definite, its trace must be negative, i.e. with $P=M+N$

$$(P+1)\left(12\sum_{i=0}^{P}h_i^2-4\right)<0 \tag{46}$$

which is satisfied by (40). Given the (average) equalizer parameter norm expansion noted in Section 4 that results in (AS) from satisfaction of (40), we conclude that no points (except the origin) in the equalizer space that maintain a negative definite Hessian can be stationary points. Therefore the local maximum at the origin is the only local maximum in the equalizer parameter space.

*Mazo class*

*Consider the (Mazo) class of stationary points typified by combined channel–equalizer impulse response coefficients $h_i$ that set $(\partial J/\partial h)=\Lambda h=0$ for $J$ the Godard cost function. The $h_i$ are either zero or of the same non-zero magnitude $1/\sqrt{(3\sigma-2)}$, where $\sigma$ is the positive number of non-zero $h_i$. When $\sigma=1$, a global minimum for $J$ is attained. When $\sigma>1$, if the associated $h$ is achievable (at least approximately) by a combined channel–equalizer in the sense described above following assumption (e), the associated stationary point cannot be a minimum, local or global, of the Godard cost function (and is therefore a saddle point).*

The result cited in italics above, which is the focus of this subsection, is valid for any channel meeting the cited restrictions and any white, zero-mean, binary ($\pm1$) source. However, for a solution of $\Lambda h=0$ involving non-zero $h_i$ with indices $i$ that are either very small or very large, it may be that (because of the length constraints on the equalizer) no equalizer tap settings can be found which correspond to these $h$.

We will begin by verifying the claim concerning the magnitude of non-zero $h_i$. Setting $\Lambda_l h_l$ to zero in (G) for each $l$ $(=0,1,2,\ldots,P)$ to achieve a stationary point requires either $h_l=0$ or $3\sum_{j=0}^{P}h_j^2-2h_l^2-1=0$. The latter condition implies

$$h_l^2=1{\cdot}5\sum_{j=0}^{P}h_j^2-0{\cdot}5 \tag{47}$$

Because the right side of (47) is independent of $l$, all non-zero $h_l$ must have the same magnitude. Assuming $\sigma$ of the $h_l$ are non-zero converts (47) to $h_l^2=1{\cdot}5\sigma h_l^2-0{\cdot}5$ or

$$h_l^2=\frac{1}{3\sigma-2} \tag{48}$$

Recall that $\sigma$ is an integer and must be one or greater for (48) to apply.

The first example of a blind equalizer exhibiting a stationary point in its cost function that results in all non-zero elements of the combined channel–equalizer impulse response being of the same magnitude is given in Reference 17 for the Sato algorithm (i.e. $\gamma_i(k+1) = \gamma_i(k) + \mu r(k-i)\{\text{sign}[y(k)] - y(k)\}$). Thus we label stationary points that set $\Lambda h$ to zero as members of the Mazo class. When there is only one non-zero $h_i$, i.e. $\sigma = 1$, in (48), $h_l^2 = 1$, which corresponds to perfect equalization. When $\sigma > 1$, we need to examine the Hessian to demonstrate that the stationary point is not a minimum.

The question of the definiteness of the Hessian can first be approached by considering, as in References 17 and 18, the special case corresponding to a channel with no dynamics, i.e. $M$ in (2) is zero. Because the $(M+N+1) \times (N+1)$ matrix $\Delta$ $(= d_0 I)$ is square when $M = 0$ and non-singular when $d_0 \neq 0$, the positive definiteness of (32) reduces to the positive definiteness of $\Psi$ in (33).[19] For the Mazo class we can rewrite (48) as

$$h_i = a_i \rho, \quad a_i \in [-1, 0, 1], \qquad \rho = \frac{1}{\sqrt{(3\sigma - 2)}} \tag{49}$$

where $\sigma > 1$ is the (integer) number of non-zero $h_i$, and so

$$\sum_{l=0}^{P} h_l^2 = \sum_{l=0}^{P} a_l^2 \rho^2 = \frac{\sigma}{3\sigma - 2} \tag{50}$$

Then (33) becomes

$$\Psi = \text{diag}(8\rho^2) + 24\rho^2 \begin{bmatrix} 0 & a_0a_1 & a_0a_2 & \cdots & a_0a_{M+N} \\ a_1a_0 & 0 & a_1a_2 & \cdots & a_1a_{M+N} \\ a_2a_0 & a_2a_1 & 0 & \cdots & a_2a_{M+N} \\ \vdots & \vdots & \vdots & \ddots & \vdots \\ a_{M+N}a_0 & a_{M+N}a_1 & a_{M+N}a_2 & \cdots & 0 \end{bmatrix} = 8\rho^2 Q \tag{51}$$

where

$$Q = \begin{bmatrix} 1 & 3a_0a_1 & 3a_0a_2 & \cdots & 3a_0a_{M+N} \\ 3a_1a_0 & 1 & 3a_1a_2 & \cdots & 3a_1a_{M+N} \\ 3a_2a_0 & 3a_2a_1 & 1 & \cdots & 3a_2a_{M+N} \\ \vdots & \vdots & \vdots & \ddots & \vdots \\ 3a_{M+N}a_0 & 3a_{M+N}a_1 & 3a_{M+N}a_2 & \cdots & 1 \end{bmatrix} \tag{52}$$

If and only if $Q$ is positive definite will $\Psi$ be positive definite. $Q$ is positive definite if and only if all its principal minors are positive definite. Because $\sigma > 1$, there exist two $a_i$, say $a_l$ and $a_J$, which are non-zero. The $2 \times 2$ principal minor of $Q$ given by

$$\begin{bmatrix} 1 & 3a_la_J \\ 3a_la_J & 1 \end{bmatrix} \tag{53}$$

has determinant $1 - 9a_l^2a_J^2$. Because the non-zero $a_l$ and $a_J$ are either plus or minus one as indicated in (49), the determinant of this principal minor is $-8$. Therefore $Q$ is not positive definite. Thus, when $M = 0$ and $\sigma > 1$ (so $N > 0$), none of the Mazo class stationary points of (AS) is stable.

When $M > 0$, we will resort to consideration of the perturbational equation form of Taylor's theorem (as stated in Sect. 10.3 of Reference 20)

$$J(h + \xi) = J(h) + \left(\frac{\partial J(c)}{\partial c}\right)^{T}\xi + \xi^{T}\left(\frac{\partial^2 J(c)}{\partial c^2}\right)\xi \tag{54}$$

Consider (54) in the vicinity of an equalizer parametrization $\bar{c}$ that is a stationary point so the gradient $(\partial J(c)/\partial c)|_{c=\bar{c}} = 0$ and

$$J(\bar{c} + \xi) = J(\bar{c}) + \xi^{T}\left(\left.\frac{\partial^2 J(c)}{\partial c^2}\right|_{c=\bar{c}}\right)\xi \tag{55}$$

where $(\partial^2 J(c)/\partial c^2)|_{c=\bar{c}}$ is the Hessian at the stationary point $\bar{c}$. If this stationary point is a minimum, then $J(\bar{c}+\xi) > J(\bar{c})$, which requires that $\xi^{T}((\partial^2 J(c)/\partial c^2)|_{c=\bar{c}})\xi \geq 0$. Because $(\partial^2 J(c)/\partial c^2)|_{c=\bar{c}}$ corresponds to $\Delta^{T}\Psi\Delta$, we can rewrite $\xi^{T}((\partial^2 J(c)/\partial c^2)|_{c=\bar{c}})\xi$ as $(\Delta\xi)^{T}\Psi(\Delta\xi)$. The scalar$(\Delta\xi)^{T}\Psi(\Delta\xi)$ must be positive for all possible non-zero $\xi$ in order for $\Delta^{T}\Psi\Delta$ to be positive definite.[19]

Now suppose that the equalizer parametrization $\bar{c}$ is such that, for the channel $\Delta$ in question, $h = \Delta\bar{c}$ is in the Mazo class with $\sigma > 1$ non-zero entries. Define $\xi_A$ to be that equalizer setting which would generate a combined channel–equalizer impulse response $h_A = \Delta\xi_A$ with zeros in all entries except $I_1$ and $I_2$, with $I_1$ and $I_2$ corresponding to the first two non-zero locations of the Mazo class stationary point $h$ under consideration. Assume first that for $\xi_A$ these two non-zero entries of $h_A$ at $I_1$ and $I_2$ are both positive, i.e. $1/\sqrt{(3\sigma - 2)}$. Define $\xi_B$ to be that equalizer setting which would generate a combined channel–equalizer impulse response $h_B = \Delta\xi_B$ that is zero at all entries except $I_2$ where it has the value $-2/\sqrt{(3\sigma - 2)}$. Our carefully crafted $\xi$ is the scaled sum of $\xi_A$ and $\xi_B$: $\xi = \delta(\xi_A + \xi_B)$. Thus $\Delta\delta(\xi_A + \xi_B)$ has only two non-zero entries: $\delta/\sqrt{(3\sigma - 2)}$ at location $I_1$ and $-\delta/\sqrt{(3\sigma - 2)}$ at location $I_2$. This choice for $\Delta\xi$ will pick out a $2 \times 2$ submatrix of $\Psi$ in the sense that $(\Delta\xi)^{T}\Psi(\Delta\xi)$ will assume a value depending on a $2 \times 2$ submatrix of $\Psi$ and no other part of $\Psi$. With $\alpha_{I_1}$ and $\alpha_{I_2}$ of the candidate Mazo class stationary point assumed to be of the same sign, the off-diagonal entries in the $2 \times 2$ submatrix of $\Psi$ picked out by $\Delta\delta(\xi_A + \xi_B)$ are both positive and

$$\delta^2(\xi_A + \xi_B)^{T}\Delta^{T}\Psi\Delta(\xi_A + \xi_B) = 8\rho^2\delta^2\begin{bmatrix} \dfrac{1}{\sqrt{(3\sigma-2)}} & \dfrac{-1}{\sqrt{(3\sigma-2)}} \end{bmatrix}\begin{bmatrix} 1 & 3 \\ 3 & 1 \end{bmatrix}\begin{bmatrix} 1/\sqrt{(3\sigma-2)} \\ -1/\sqrt{(3\sigma-2)} \end{bmatrix} = -32\delta^2 \tag{56}$$

which is not positive. Thus the associated Hessian is not positive definite. If $\alpha_{I_1}$ and $\alpha_{I_2}$ are of different sign in the candidate Mazo class stationary point under consideration, our test $\xi$ can be reduced to just $\delta\xi_A$. The resulting $\Delta\delta\xi_A$ is$[1/\sqrt{(3\sigma-2)} \; -1/\sqrt{(3\sigma-2)}]$ and $(\delta\Delta\xi)^{T}\Psi(\delta\Delta\xi) = \delta^2\xi_A^{T}\Delta^{T}\Psi\Delta\xi_A = -32\delta^2$ as before. Actually, there will almost never be equalizer settings $\xi_A$ and $\xi_B$ which exactly give $h_A$ and $h_B$ of the prescribed type. However, with sufficiently long equalizers these values can at least be closely approximated. Accordingly, the quadratic form based on the Hessian will still be negative.

The conclusion that can be drawn from these special cases is that for whatever finite $M$ and $\sigma > 1$, none of the Mazo class stationary points of (AS) is stable. Only when the channel–equalizer combination has one non-zero impulse response coefficient ($\sigma = 1$ and (56) does not apply) can the Hessian be positive definite as desired.

While this result echoes that of Reference 3, the difference is that in Reference 3 the equalizer is assumed infinite-dimensional and here we have established the lack of false minima among the Mazo class equilibria for long, but finite-length, equalizers.

*Ding class*

*Consider the (Ding) class of stationary points in the equalizer parameter space that place the partial of the Godard cost function J with respect to the combined channel–equalizer impulse response vector h ($\partial J/\partial h = \Lambda h$) in the non-trivial nullspace of the channel impulse response matrix $\Delta^T$. For sufficiently long equalizers, entries near the middle of the vector $\partial J/\partial h$ must be near zero for stationary points in this class, as they are for the Mazo class as well.*

We now consider the situation where $\Lambda h$ is a non-zero vector in the nullspace of $\Delta^T$. Note that the Mazo class is trivially in the nullspace (with $\Lambda h = 0$). The first explication of ill-convergence of the Godard algorithm due to a non-zero $\Lambda h$ being in the nullspace of $\Delta^T$ is provided in Reference 7. We label stationary points that zero (G) with $\Lambda h \neq 0$ as members of the Ding class. We will now analyse the structure of such vectors.

Owing to the $(N+1)\times(M+N+1)$ dimensions of $\Delta^T$, its nullspace has a basis set of $M$ column vectors of length $M+N+1$. For the $d_i$ in $\Delta$ in (23), define the roots of

$$d_0 z^M + d_1 z^{M-1} + d_2 z^{M-2} + \cdots + d_{M-1} z + d_M = 0 \tag{57}$$

as $\lambda_i$ for $i = 1, 2, \ldots, M$. For $M$ roots, $d_0 \neq 0$. Recall that by assumption (e) there are no roots on the unit circle, i.e. $|\lambda_i| \neq 1\ \forall i$. We will divide the roots of (57) into two groups: (i) inside the unit circle $|\lambda_1|, |\lambda_2|, \ldots, |\lambda_q| < 1$ and (ii) outside the unit circle $|\lambda_{q+1}|, |\lambda_{q+2}|, \ldots, |\lambda_M| > 1$. For simplicity we will assume that the $\lambda_i$ are distinct. From (23) and (57)

$$\Delta^T[\lambda_i^{M+N}\ \lambda_i^{M+N-1}\ \ldots\ \lambda_i^2\ \lambda_i\ 1]^T = 0 \tag{58}$$

and

$$\Delta^T[1\ \lambda_i^{-1}\ \lambda_i^{-2}\ \ldots\ \lambda_i^{-M-N+1}\ \lambda_i^{-M-N}]^T = 0 \tag{59}$$

If (58) is applied only to the roots from group (i) with smaller-than-unity magnitude and (59) is only applied to values of $\lambda_i$ from group (ii) with larger-than-unity magnitude, the entries in the vectors multiplying $\Delta^T$ in both (58) and (59) will be bounded in magnitude by unity no matter how large $M$ or $N$ might be. Now the vectors $[\lambda_i^{M+N}\ \lambda_i^{M+N-1}\ \ldots\ \lambda_i^2\ \lambda_i\ 1]^T$ and $[1\ \lambda_i^{-1}\ \lambda_i^{-2}\ \ldots\ \lambda_i^{-M-N+1}\ \lambda_i^{-M-N}]^T$ are null vectors of $\Delta^T$ and there are $M$ of them. They are linearly independent, since the roots are distinct. Thus, the $M$ null vectors span the nullspace of $\Delta^T$.

Hence, if $\bar{h}$ is such that $\Delta^T \Lambda h = 0$ with $\Lambda h \neq 0$, it follows that for some set of coefficients $\beta_i$ with $i \in [1, 2, \ldots, M]$,

$$\Lambda h = \sum_{i=1}^{q} \beta_i \begin{bmatrix} \lambda_i^{M+N} \\ \lambda_i^{M+N-1} \\ \vdots \\ \lambda_i^2 \\ \lambda_i \\ 1 \end{bmatrix} + \sum_{i=q+1}^{M} \beta_i \begin{bmatrix} 1 \\ \lambda_i^{-1} \\ \lambda_i^{-2} \\ \vdots \\ \lambda_i^{-M-N+1} \\ \lambda_i^{-M-N} \end{bmatrix} \tag{60}$$

For $N$ very large the last $q$ rows of (60) can be written as

$$\Lambda h\big|_{\text{last } q \text{ rows with } N \text{ large}} = \begin{bmatrix} \lambda_1^{q-1} & \lambda_2^{q-1} & \ldots & \lambda_q^{q-1} \\ \lambda_1^{q-2} & \lambda_2^{q-2} & \ldots & \lambda_q^{q-2} \\ \vdots & \vdots & & \vdots \\ 1 & 1 & \ldots & 1 \end{bmatrix} \begin{bmatrix} \beta_1 \\ \beta_2 \\ \vdots \\ \beta_q \end{bmatrix} \tag{61}$$

Similarly, for $N$ very large the first $M-q$ rows of (60) can be written as

$$\Lambda h\big|_{\text{first } M-q \text{ rows with } N \text{ large}} = \begin{bmatrix} 1 & 1 & \cdots & 1 \\ \lambda_{q+1}^{-1} & \lambda_{q+2}^{-1} & \cdots & \lambda_M^{-1} \\ \vdots & \vdots & & \vdots \\ \lambda_{q+1}^{-M-1} & \lambda_{q+2}^{-M-1} & \cdots & \lambda_M^{-M-1} \end{bmatrix} \begin{bmatrix} \beta_{q+1} \\ \beta_{q+2} \\ \vdots \\ \beta_M \end{bmatrix} \tag{62}$$

In both (61) and (62) the square matrix filled with $\lambda_i$ is a Vandermonde matrix, which (in this case of distinct $\lambda_i$) has a strictly non-zero determinant.[21] Because, as shown in Section 4, all stationary points occur in a bounded region of the $h$-space, $\Lambda h$ is bounded. Thus, with the determinants of the Vandermonde matrices in (61) and (62) non-zero, the $\beta_i$ are bounded. Then, if $N$ is large (enough), (60) shows that entries near the middle of $\Lambda h$ must be approximately zero. The distance from either end needed to claim that the magnitude of a particular entry of $\Lambda h$ is below some $\varepsilon$ can be upper bounded. If the $\lambda_i$ are not distinct, a similar result can be based on generalized Vandermonde matrices.

Having established that $(\Lambda h)_i$ can be significantly different from zero only for values of $i$ corresponding to the first few or last few vector entries, we now examine the consequences for the values of $h_i$ associated with small $|\Lambda_j h_i|$. Recalling (20), i.e. $\Lambda_j = 4(3\sum_{l=0}^{P} h_l^2 - 1 - 2h_j^2)$, we conclude that a small $|\Lambda_j h_i|$ implies a small $|h_i|$ unless

$$3\sum_{l=0}^{P} h_l^2 - 1 - 2h_j^2 \approx 0 \tag{63}$$

Suppose there are $\sigma$ values of $h_i$ for which (63) holds. Then, they are necessarily all of approximately the same magnitude, i.e. $\frac{1}{2}(3\sum_{l=0}^{P} h_l^2 - 1)^{1/2}$. With $\sigma \geq 2$ the same argument as used for the Mazo equilibrium analysis reveals that the associated equilibrium is not stable. On the other hand, a minimum with $\sigma = 1$ cannot be ruled out.

Hence the Ding equilibria involve combined channel–equalizer impulse responses with significant values of $h$ at the beginning or end of the available tap span (or both) and one or more significant intermediate values. However, there will be no more than one such intermediate value if the equilibrium is to be stable. That there are stable equilibria in the Ding class is established in References 5–7. The examples in References 5 and 7 are for situations where the length of the equalizer is shorter than in our assumption (e). The example in Reference 6 accommodates an arbitrarily long equalizer, with significant entries of $h$ limited to one end as is the associated $c$. However, so far, no stable equilibria in the Ding class for extremely long, but finite-length, equalizers with a lopsided tap energy distribution have been documented that also include a single significant value in the mid-range of the achieved $h$.

## 6. ESTABLISHING A REGION OF ATTRACTION

*Consider an arbitrary point in the equalizer parameter space and the ray from the origin passing through that point. If at the point the Hessian is positive definite, it remains positive definite at all subsequent points further from the origin on the ray.*

For a particular $c$, which creates a specific $h = \Delta c$, assume that the Hessian $\Delta^T \Psi \Delta$ in (H) is positive definite. Now consider the extension of $c$ along a ray as $\alpha c$, where $\alpha > 1$. Because $\alpha$ is a scalar, $\Delta(\alpha c) = \alpha \Delta c = \alpha h$. Given (32),

$$\Psi(\alpha h) = \alpha^2 \Psi(h) + (\alpha^2 - 1)4I \tag{64}$$

Because $\Psi(h)$ is positive definite, both addends on the right side of (64) are positive definite (as long as $\alpha > 1$) and their sum is positive definite.[22] Thus $\Psi(\alpha h)$ is positive definite as claimed.

By a similar argument, once the Hessian is negative definite, for all points closer to the origin ($\alpha < 1$) on a ray from the origin the Hessian remains negative definite. A similar argument also applies to the sign definiteness of the gradient vector.

Convex sets in the $c$-space with positive definite Hessians ($\partial^2 J/\partial c^2$) throughout are an important ingredient in a fundamental property of descent algorithms.[20] If a function $J$ is being minimized over a convex set, if the trajectories of a descent algorithm point inwards at all boundary points of the set and if the Hessian $\partial^2 J/\partial c^2$ is positive throughout the set, then there is a unique minimum in the region. Thus any trajectory starting anywhere in the region or on its boundary leads to this minimum. Recall that our minimization is over the equalizer parameter space (rather than the combined channel–equalizer parameter space).

To examine implications of the observation at the start of this section, reconsider Figures 4–7. Each of the minima in Figure 4 is surrounded by a circle within which the Hessian is positive definite. Thus, along rays from the origin from the tangent to one side to the tangent to the other side of this circle, from the circle on out the Hessian is positive definite. Such a convex set is illustrated about the local minimum near $c_0 = 0$ and $c_1 = 1{\cdot}1$ in the shaded region in Figure 9. The segment labelled $a$ is the arc from a circle centred on the local minimum within which the Hessian is positive definite. Refer to Figure 7 to assess the size of this circle (which has a diameter of less than 0·4). The segments $b$ and $c$ are the tangent rays to the circle.

Such a convex set of infinite extent with a positive definite Hessian throughout need not have all trajectory motions inward from boundary points. Overlay the shaded region of Figure 9 on the angular motion plot of Figure 6. Note how for sufficiently large equalizer parametrizations the angular motion on both segments $b$ and $c$ is always in one direction: clockwise. Thus, if the trajectories point inwards on one side of the candidate convex region, they point outwards on the other.

Now we will construct a convex set about the global minimum in the vicinity of $(c_0, c_1) = -(1{\cdot}6, 0{\cdot}9)$ that has positive definite Hessian throughout and trajectories pointing inwards on all boundaries. From Figure 6 we see that we can draw a vertical line along $c_0 = -1{\cdot}4$ from $c = -1$ to the border between clockwise and counterclockwise angular motion, which occurs between $c_0 = -0{\cdot}8$ and $-0{\cdot}6$. Consider the convex set (which includes the global minimum) that is in the shadow cast out to some radius by this vertical line segment due to a

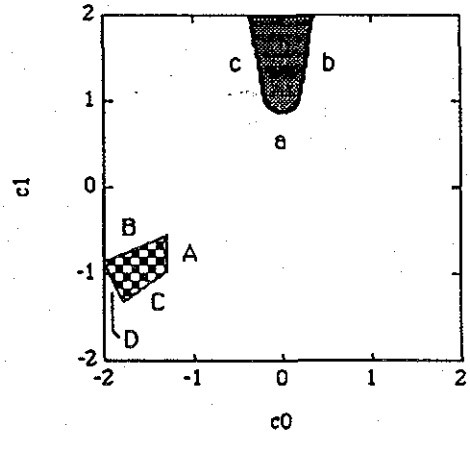


Figure 9. Special regions about local minima

point source at the origin, as illustrated as the checkered region in Figure 9. From Figures 5 and 6 all points along the segment $A$ have outward radial motion and clockwise angular motion. Thus along the segment $A$ of the boundary the trajectories point into the convex set of interest. From Figure 6 the trajectories along the rays bounding this convex set, i.e. segments $B$ and $C$, also point into this set. That is why the construction of segment $A$ tops out at the clockwise/counterclockwise boundary in Figure 6. The segment $D$ is an arc from a circle centred at the origin, and the radial motion along it, as seen from Figure 5, is inward. Thus the checkered set in Figure 9, is a convex set with positive definite Hessian throughout and inward-pointing trajectories on all boundaries, i.e. a conservative subset of the region of attraction of the contained global minimum. This convex set does not include any portion of either axis. Thus a more sophisticated construction would be needed to validate a single-spike initialization.

## 7. CONCLUSIONS

Averaging theory[12,13] indicates that for a suitably small step size the actual adaptive equalizer algorithm of (5) closely follows the behaviour of (AS). (AS) has stationary points where (G) is zeroed that are minima if (H) is positive definite. (AS), (G) and (H) are defined at the close of Section 3. Some significant features described in this paper of the Godard error surface descended by (AS) include the following:

(A) A sufficiently large (small) equalizer parametrization will result in equalizer parameter power contraction (expansion).
(B) The only local maximum is at the origin of the equalizer parameter space.
(C) No Mazo class stationary points, except those with globally optimal behaviour, are stable stationary points of the average behaviour of the Godard algorithm with a sufficiently long (but finite-length) equalizer.
(D) For sufficiently long (but finite-length) equalizers the Ding class of stationary points, which includes all the false local minima, must zero the centre of the partial derivative of the Godard cost function with respect to the combined channel–equalizer impulse response coefficient vector. For such equilibria to be stable, no more than one term near the middle of the combined channel–equalizer impulse response can be non-zero.
(E) Along any ray from the origin in the equalizer parameter space, once the Hessian becomes positive (negative) definite, it remains positive (negative) definite for equalizer parametrizations further from (closer to) the origin along the same ray.

While these results fall short of adequately characterizing the Godard error surface so the utility of any initialization scheme can be assessed, they represent the first set of results regarding Godard error surface topology in terms of the 'shape' of the gradient and Hessian specifically accumulated to assist that effort. It is important to recognize that our results depend on the specific operating conditions presumed in Section 1. For example, if one forfeits the assumption of a sequentially decorrelated source, point (C) above is no longer true.[23]

Our analysis provides some support for initialization with a large centre spike and otherwise small values. One can demonstrate that from such an initialization of a very long equalizer it takes some time for taps more distant from the centre tap to become non-zero. Capture by an equilibrium in a finite time would be tantamount to a restraint on the magnitude of the outer taps, especially of a very long equalizer. This could exclude the possibility that the equilibrium reached in finite time would be in the Ding class. Furthermore, the only possible Mazo equilibria are the ones with global performance. Thus global asymptotic optimality ensues. One expectation is that initially suppressing the potential growth rate of the outer taps could enhance

the likelihood of success by effectively allowing more time before capture by a false minimum could occur given (D). This suppression could be achieved by relating step size inversely to the distance along the equalizer tap delay line from the centre tap or by delaying the switching of each tap's step size from zero to its fixed non-zero value at a time after start-up that is monotonically non-decreasing with distance from the centre tap. However, one cannot yet demonstrate that convergence to within a suitably small region about an equilibrium will occur in bounded time.

These observations complement the result in Reference 24 (p. 131), which indicates that if the tails of a long equalizer are small, only global minima exist. However, again no proof yet exists that guarantees that the acquired local minima in the $c$-space have small outer taps for any particular initialization strategy no matter how long the finite-length equalizer.

The characteristics of the Godard cost function that apply to $(N+1)$-dimensional equalizers for $N>1$ were the focus of this paper. However, one way this research can be advanced is through the recognition of topological features in low-dimensional examples and the formulation and testing of conjectures regarding their extendibility to higher dimensions. Indeed, we used a single two-dimensional $(N=1)$ example to illustrate several of the observations made in this paper. A useful image of the Godard cost function that arises with the examination of such two-dimensional cases is of asombrero with the minima on the rim and the local maximum in the centre. Other observed similarities can be turned into the following higher-dimensional conjectures:

(F) The rotational direction of average motion in any plane containing the origin can only change once along each ray from the origin. (This could help advance the region of attraction construction.)

(G) A point exists on at least one co-ordinate axis in the equalizer parameter space such that the infinite segment of the axis beyond this point is in a convex region of attraction of a local minimum with globally optimal performance. (This could help refine the single-spike initialization procedure.)

This paper focused exclusively on a baud-spaced equalizer adapted by the Godard (or constant modulus) algorithm. For a baud-spaced equalizer the input sample period $T$, and therefore the unit delay in this baud- (or $T$-) spaced tapped-delay-line equalizer, equals the baud period, i.e. the time between source symbols. In practice with analogue transmission and channels, fractionally spaced equalizers are used with the equalizer input sample period less than the baud sample period. As recently discovered,[25] this implementation offers dramatically improved global convergence possibilities. However, under certain conditions on the channel dynamics[26] the performance of the fractionally spaced equalizer can collapse to that of a baud-spaced equalizer as studied in this paper.

## ACKNOWLEDGEMENTS

C.R.J. was supported by NSF Grant ECS-9022785 and Applied Signal Technology, Inc. The Cooperative Research Centre is supported by the Australian Government under the Cooperative Research Centre Program.

## REFERENCES

1. Godard, D. N., 'Self-recovering equalization and carrier tracking in two dimensional data communication systems', *IEEE Trans. Commun.*, COM-28, 1867–1875 (1980).
2. Treichler, J. R. and B. G. Agee, 'A new approach to multipath correction of constant modulus signals', *IEEE Trans. Acoust., Speech, Signal Process.*, ASSP-31, 459–472 (1983).

3. Foschini, G. J., 'Equalizing without altering or detecting data', *AT&T Tech. J.*, **64**, 1885–1911 (1985).
4. Shalvi, O. and E. Weinstein, 'New criteria for blind deconvolution of nonminimum phase systems (channels)', *IEEE Trans. Info. Theory*, **IT-36**, 312–321 (1990).
5. Ding, Z., R. A. Kennedy, B. D. O. Anderson and C. R. Johnson Jr., 'Ill-convergence of Godard blind equalizers in data communication systems', *IEEE Trans. Commun.*, COM-39, 1313–1327 (1991).
6. Ding, Z. and C. R. Johnson Jr., 'On the non-vanishing stability of undesirable equilibria for FIR Godard blind equalizers', *IEEE Trans. Signal Process.*, **41**, 1940–1944 (1993).
7. Ding, Z., C. R. Johnson Jr. and R. A. Kennedy, 'On the (non)existence of undesirable equilibria of Godard blind equalizers', *IEEE Trans. Signal Process.*, **40**, 2425–2432 (1992).
8. Johnson Jr., C. R., 'Admissibility in blind adaptive channel equalization', *IEEE Control Syst. Mag.*, **11**, 3–15 (1991).
9. Kennedy, R. A., K. Yamazaki, Z. Ding, S. Verdú and S. Vembu, 'Approaches to blind equalization: open problems', *Proc. 4th IFAC Int. Symp. on Adaptive Systems in Control and Signal Processing*, Grenoble, July 1992, pp. 627–632.
10. Bellini, S., 'Bussgang techniques for blind deconvolution and equalization', in Haykin, S. (ed.), *Blind Deconvolution*, Prentice-Hall, Englewood Cliffs, NJ, 1994, pp. 8–59.
11. Johnson Jr., C. R., S. Dasgupta and W. A. Sethares, 'Averaging analysis of local stability of a real constant modulus algorithm adaptive filter', *IEEE Trans. Acoust., Speech, Signal Process.*, ASSP-36, 900–910 (1988).
12. Anderson, B. D. O., R. R. Bitmead, C. R. Johnson Jr., P. V. Kokotovic, R. L. Kosut, I. M. Y. Mareels, L. Praly and B. D. Riedle, *Stability of Adaptive Systems: Passivity and Averaging Analysis*, MIT Press, Cambridge, MA, 1986.
13. Solo, V. and X. Kong, *Adaptive Signal Processing Algorithms: Stability and Performance*, Prentice-Hall, Englewood Cliffs, NJ, 1995.
14. Ding, Z. and R. A. Kennedy, 'On the whereabouts of local minima for blind adaptive equalizers', *IEEE Trans. Cir. Syst. II*, **39**, 119–123 (1992).
15. Haykin, S., *Adaptive Filter Theory*, 2nd edn, Prentice-Hall, Englewood Cliffs, NJ, 1991, Sect. 9.13.
16. Bellanger, M. G., *Adaptive Digital Filters and Signal Analysis*, Marcel Dekker, New York, 1987, Sect. 3.9.
17. Mazo, J. E., 'Analysis of decision-directed equalizer convergence', *Bell Syst. Tech. J.*, **59**, 1857–1876 (1980).
18. Johnson Jr., C. R., P. C. E. Bennett, J. P. LeBlanc and V. Krishnamurthy, 'Blind adaptive equalizer average stationary point stability with admissibility consequences', *Proc. 26th Conf. on Information Sciences and Systems*, Princeton, NJ, March 1992, pp. 727–732.
19. Strang, G., *Linear Algebra and Its Applications*, 2nd edn, Academic, New York, 1980, Sect. 6.2.
20. Luenberger, D. G., *Introduction to Linear and Nonlinear Programming*, Addison-Wesley, Reading, MA, 1973.
21. Kailath, T., *Linear Systems*, Prentice-Hall, Englewood Cliffs, NJ, 1980, p. 649.
22. Noble, B., *Applied Linear Algebra*, Prentice-Hall, Englewood Cliffs, NJ, 1969, p. 417.
23. Johnson Jr., C. R., J. P. LeBlanc and V. Krishnamurthy, 'Godard blind equalizer misbehavior with correlated sources: two examples', *J. Maroc. Automat. Info. Trait. Signal*, **2**, 1–39 (1993).
24. Shalvi, O. and E. Weinstein, 'Universal methods for blind deconvolution', in Haykin, S. (ed.), *Blind Deconvolution*, Prentice-Hall, Englewood Cliffs, NJ, 1994, pp. 121–180.
25. Fijalkow, I., F. López de Victoria and C. R. Johnson Jr., 'Adaptive fractionally spaced blind equalization', *Proc. 6th IEEE DSP Workshop*, Yosemite, CA, October 1994, IEEE, New York, 1994, pp. 257–260.
26. Fijalkow, I., J. R. Treichler and C. R. Johnson Jr., 'Fractionally spaced blind equalization: loss of channel disparity', *Proc. 1995 IEEE Int. Conf. on Acoustics, Speech, and Signal Processing*, Detroit, MI, May 1995, IEEE, New York, 1995.